Control Engineering Practice 21 (2013) 1302–1309

Contents lists available at SciVerse ScienceDirect

Control Engineering Practice

journal homepage: www.elsevier.com/locate/conengprac

A nonlinear trajectory tracking controller for mobile robots with velocity limitation via fuzzy gains

Cassius Z. Resende [a,*,1], Ricardo Carelli [b], Mário Sarcinelli-Filho [a]

[a] Department of Electrical Engineering, Federal University of Espírito Santo (UFES), Av. Fernando Ferrari, 514, 29075-910, Vitória, ES, Brazil
[b] Institute of Automatics (INAUT), National University of San Juan (UNSJ), Av. San Martin Oeste 1109, 5400 San Juan, Argentina

ARTICLE INFO

Article history:
Received 28 December 2012
Accepted 29 May 2013

Keywords:
Robotics
Mobile robots
Autonomous vehicles
Fuzzy control
Takagi–Sugeno model
Nonlinear control systems

ABSTRACT

This paper proposes a fuzzy controller for trajectory tracking with unicycle-like mobile robots. Such controller uses two Takagi–Sugeno (TS) fuzzy blocks to generate its gains. The controller is able to limit the velocity and control signals of the robot, and to reduce the errors arising from its dynamics as well. The stability of the developed controller is proven, using the theory of Lyapunov. Experimental results show that the use of the proposed controller is attractive in comparison with the use of a controller with fixed saturation function.

1. Introduction

This work proposes a new approach to limit the control signals during a trajectory tracking with unicycle-like mobile robots. In the literature it is common to find works that use explicit saturation functions such as the hyperbolic tangent to limit control signals (Andaluz, Roberti, Toibero, & Carelli, 2012; Martins, Celeste, Carelli, Sarcinelli-Filho, & Bastos-Filho, 2008). In this work, however, fuzzy rules are adopted to achieve such limitation while keeping an efficient trajectory tracking controller operation.

The fuzzy control emerged in the 70s as a heuristic method based on the knowledge of the designer about the process to be controlled. Such method started being adopted after the publication of the works of Zadeh (1973) and Mamdani (1974). This methodology has the advantage of controlling a plant without an explicit knowledge of its dynamics. However, to prove the stability of the closed-loop control system using these controllers is a difficult task. In the field of mobile robots control, for instance, several works have used the heuristic methodology to design fuzzy controllers, without studying the system stability (Antonelli, Chiaverini, & Fusco, 2007; Deist & Fourie, 1993; Hung & Chung, 2006; Lakehal, Amirat, & Pontnau, 1995; Susnea, Filipescu, Vasiliu, & Filipescu, 2008). This means that there is no theoretical guarantee that the task being performed will be accomplished accordingly.

Due to the need of a formal proof of stability for the control system, fuzzy controllers have obtained a new focus with the Takagi–Sugeno (TS) fuzzy controllers (Takagi & Sugeno, 1985). Tanaka and Sugeno (1992) showed that the TS fuzzy controllers can be designed rigorously, following methodologies that can be reproduced consistently, guaranteeing the system stability and using several performance criteria. The technique most commonly adopted for the design of controllers represented as a TS fuzzy model is the Parallel Distributed Compensation (PDC) (Wang, Tanaka, & Griffin, 1996). This technique has been used successfully to design controllers for trajectory tracking with mobile robots (Guechi, Lauber, Dambrine, Klancar, & Blazic, 2010; Guechi, Abellard, & Franceschi, 2012) and to solve the backing control problem of a mobile robot with multiple trailers (Tanaka, Kosaki, & Wang, 1998). Nevertheless, it is important to emphasize that although the PDC technique is based on fuzzy models, this design methodology does not use the knowledge of the designer about the process.

The controller here proposed uses the control structure reported in Resende, Espinosa, Bravo, Sarcinelli-Filho, and Bastos-Filho (2011), combining the heuristic knowledge of the problem, the sector nonlinearity approach (Tanaka & Wang, 2001) and the inverse kinematic of the mobile platform. The use of the sector nonlinearity allows designing a fuzzy controller with a quite reduced number of rules and a quite low complexity, making it suitable for implementation in the low-profile processors generally available onboard mobile platforms.

Through the application of the inverse kinematic of the mobile platform, it was possible to design a TS fuzzy controller guaranteeing the stability of the closed loop system, but without using the PDC technique. More than this, it was possible to use the heuristic knowledge to reduce position errors caused by the difference

* Corresponding author. Tel.: +55 2740092684; fax: +55 2740092644.
E-mail addresses: cassius@ifes.edu.br (C.Z. Resende), rcarelli@inaut.unsj.edu.ar (R. Carelli), mario.sarcinelli@ufes.br (M. Sarcinelli-Filho).
[1] On leave from the Federal Institute for Education, Science and Technology of Espírito Santo (IFES), Serra, ES, Brazil.

0967-0661/$ - see front matter © 2013 Elsevier Ltd. All rights reserved.
http://dx.doi.org/10.1016/j.conengprac.2013.05.012

between the desired values of linear and angular velocities (system inputs) and the current velocity values assumed by the mobile platform.

Three experiments run using a unicycle-like mobile robot are reported here, which have shown that the proposed controller performs better than the similar controller proposed by Martins et al. (2008). It is worth mentioning that the proposed controller can be adapted to other mobile platforms, demanding just the knowledge of its inverse kinematic.

To develop and validate the proposed controller, the paper is hereinafter organized in four sections. Section 2 presents the kinematic model of the unicycle-like mobile robot, while Section 3 details the proposed nonlinear controller with variable gains and discusses the system stability. In the sequel, Section 4 shows the experimental results and performance comparisons between the two aforementioned controllers. Finally, Section 5 highlights some conclusions.

2. The kinematic model adopted

Traditionally, in the motion control of unicycle-like mobile robots, the robot is considered as a point located at the middle of the virtual axle. In this work, however, the point that should follow a predetermined trajectory is located in front of the virtual axle (point d of Fig. 1). Such point is hereinafter named as the point of interest.

From Fig. 1, the velocity of the point of interest with respect to the inertial frame $\{I\}$ is given by

$$\begin{bmatrix}\dot{x}\\ \dot{y}\end{bmatrix}=\begin{bmatrix}\cos\psi & -a\sin\psi\\ \sin\psi & a\cos\psi\end{bmatrix}\begin{bmatrix}u\\ \omega\end{bmatrix}=\mathbf{C}\begin{bmatrix}u\\ \omega\end{bmatrix}, \tag{1}$$

where the linear velocity u and the angular velocity ω are the control inputs of the robot, $\dot{x}$ and $\dot{y}$ are, respectively, the velocity of the point of interest in the X and Y directions of the inertial frame, $a>0$ represents the distance between the point of interest and the center of the virtual axle, and ψ is the orientation of the robot, which is given by the solution of $\dot{\psi}=\omega$.

The appropriate values of u and ω to impose desired velocities $\dot{x}$ and $\dot{y}$ to the point of interest are determined by the inverse kinematics (Martins et al., 2008)

$$\begin{bmatrix}u\\ \omega\end{bmatrix}=\begin{bmatrix}\cos\psi & \sin\psi\\ -\frac{1}{a}\sin\psi & \frac{1}{a}\cos\psi\end{bmatrix}\begin{bmatrix}\dot{x}\\ \dot{y}\end{bmatrix}=\mathbf{C}^{-1}\begin{bmatrix}\dot{x}\\ \dot{y}\end{bmatrix}, \tag{2}$$

where $\mathbf{C}^{-1}$ is the inverse kinematics matrix. Unlike the middle point of the virtual axle, the point of interest d does not have any velocity restriction in the robot workspace (such point can move in any direction).

3. The nonlinear trajectory tracking controller with fuzzy gains

3.1. The control law

During the trajectory tracking, the point of interest of the robot shall follow a programmed trajectory defined by an equation like $p(t)=(x_D(t),y_D(t))$, where (x_D,y_D) is the point to be followed and $t\geq 0$ is the time variable. To comply with this control objective, this work proposes the control law

$$\begin{bmatrix}u_r\\ \omega_r\end{bmatrix}=\mathbf{C}^{-1}\left(\begin{bmatrix}\dot{x}_D\\ \dot{y}_D\end{bmatrix}+\begin{bmatrix}\nu_x\\ \nu_y\end{bmatrix}\right), \tag{3}$$

where u_r and ω_r are the controller outputs which are, respectively, the linear and angular reference velocities; $\dot{x}_D$ and $\dot{y}_D$ are, respectively, the velocity of the programmed trajectory at the point (x_D,y_D) in the X and Y directions of the inertial frame; and ν_x and ν_y are the outputs of two "fuzzy velocity compensators" (FVC).

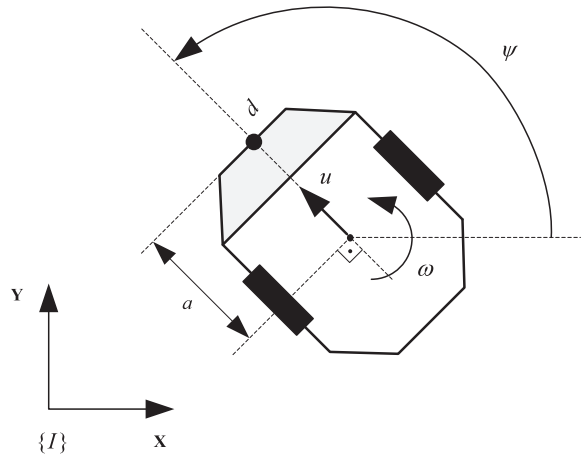

Fig. 1. The unicycle-like mobile robot and its kinematic parameters.

According to Fig. 2, the idea of the proposed controller is that once the point of interest d coincides with the desired point (x_D,y_D) at the trajectory, the reference velocities $\dot{x}_r$ and $\dot{y}_r$ are kept equal to the velocities of the reference trajectory, that is $\dot{x}_r=\dot{x}_D$, $\dot{y}_r=\dot{y}_D$, $\nu_x=0$ and $\nu_y=0$. Upon the occurrence of position errors $\tilde{x}$ and $\tilde{y}$, the fuzzy controller generates compensation terms for the velocities (ν_x and ν_y), until the point of interest d coincides with the desired point (x_D,y_D) at the trajectory again. Notice that the matrix $\mathbf{C}^{-1}$ is responsible for transforming $\dot{x}_r$ and $\dot{y}_r$ in u_r and ω_r.

The premise variables of the fuzzy velocity compensator X (FVC_X) are $|\dot{x}_D|$ and $|\tilde{x}|$, respectively the magnitude of the velocity of the programmed trajectory and the magnitude of the position error both in the X direction. In turn, the premise variables of the fuzzy velocity compensator Y (FVC_Y) are $|\dot{y}_D|$ and $|\tilde{y}|$, respectively the magnitude of the velocity of the programmed trajectory and the magnitude of the position error both in the Y direction.

The premise variables $|\tilde{x}|$ and $|\tilde{y}|$ are divided into three fuzzy sets: small error (S), medium error (M) and large error (B). The membership function of the small error fuzzy set is given by

$$f_S(|\tilde{e}|)=\begin{cases}1, & |\tilde{e}|<\eta_1\ [\mathrm{m}];\\ \dfrac{\eta_1}{(\eta_1-\eta_2)}-\dfrac{\eta_1\cdot\eta_2}{(\eta_1-\eta_2)|\tilde{e}|}, & \eta_1\leq|\tilde{e}|<\eta_2\ [\mathrm{m}];\\ 0, & \eta_2\leq|\tilde{e}|<\eta_3\ [\mathrm{m}];\end{cases} \tag{4}$$

while the membership function of the medium error fuzzy set is given by

$$f_M(|\tilde{e}|)=\begin{cases}0, & |\tilde{e}|<\eta_1\ [\mathrm{m}];\\ \dfrac{\eta_1\cdot\eta_2}{(\eta_1-\eta_2)|\tilde{e}|}-\dfrac{\eta_2}{(\eta_1-\eta_2)}, & \eta_1\leq|\tilde{e}|<\eta_2\ [\mathrm{m}];\\ \dfrac{\eta_2}{(\eta_2-\eta_3)}-\dfrac{\eta_2\cdot\eta_3}{(\eta_2-\eta_3)|\tilde{e}|}, & \eta_2\leq|\tilde{e}|<\eta_3\ [\mathrm{m}];\end{cases} \tag{5}$$

and the membership function of the large error fuzzy set is given by

$$f_B(|\tilde{e}|)=\begin{cases}0, & |\tilde{e}|<\eta_2\ [\mathrm{m}];\\ \dfrac{\eta_2\cdot\eta_3}{(\eta_2-\eta_3)|\tilde{e}|}-\dfrac{\eta_3}{(\eta_2-\eta_3)}, & \eta_2\leq|\tilde{e}|<\eta_3\ [\mathrm{m}];\end{cases} \tag{6}$$

where $|\tilde{e}|$ represents the magnitude of the position error ($|\tilde{x}|$ or $|\tilde{y}|$). Fig. 3 presents a sketch of such membership functions.

The premise variables $|\dot{x}_D|$ and $|\dot{y}_D|$ are divided into two fuzzy sets: low velocity (L) and high velocity (H). According to Fig. 4, the membership functions of such premise variables are defined

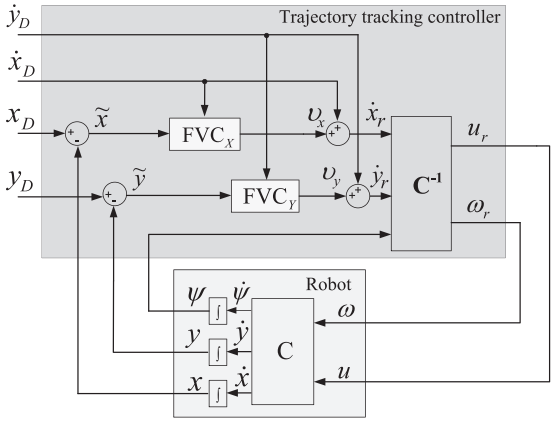

Fig. 2. Block diagram of the trajectory tracking controller with fuzzy gains.

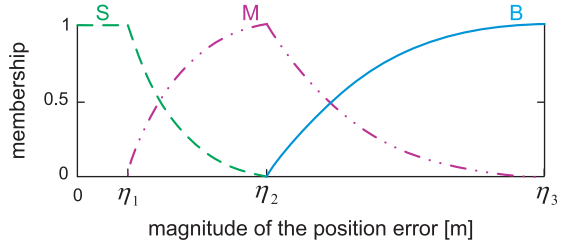

Fig. 3. Membership functions for the magnitude of the trajectory tracking errors.

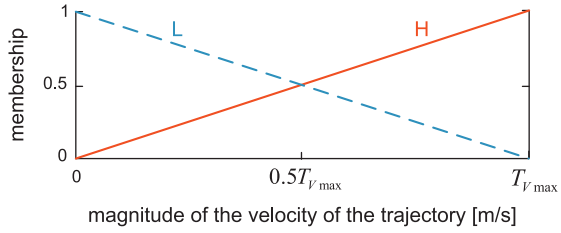

Fig. 4. Membership functions for the magnitude of the velocity of the trajectory.

from zero to T_{Vmax}, where T_{Vmax} is the limit of velocity for the programmed trajectory in the respective direction.

Table 1 presents the six rules and the six gains which compose each fuzzy velocity compensator. In such table, T_{Vmax} is the limit of velocity for the programmed trajectory in the X or Y direction, R_{Vmax} is the maximum velocity allowed for the point of interest in the X or Y direction during a trajectory tracking task and V_{pos} is the maximum velocity allowed for the point of interest in the X or Y direction during a positioning task. As examples, the first rule of the FVC$_X$, given by "Rx_1: IF $|\dot{x}_D|$ is low (L) and $|\tilde{x}|$ is small (S), THEN $\nu_x = a_1\tilde{x}$" is represented in Table 1 by "$R_1 : LS \rightarrow a_1$" and the sixth rule of the FVC$_Y$, given by "Ry_6: IF $|\dot{y}_D|$ is high (H) and $|\tilde{y}|$ is large (B), THEN $\nu_y = a_6\tilde{y}$" is represented in Table 1 by "$R_6 : HB \rightarrow a_6$".

Table 1
The six rules of the fuzzy velocity compensators.

$R_1 : LS \rightarrow a_1$ (it is chosen)	$R_4 : HS \rightarrow a_4 = \frac{R_{Vmax} - T_{Vmax}}{\eta_1}$
$R_2 : LM \rightarrow a_2 = \frac{V_{pos}}{\eta_2}$	$R_5 : HM \rightarrow a_5 = \frac{R_{Vmax} - T_{Vmax}}{\eta_2}$
$R_3 : LB \rightarrow a_3 = \frac{V_{pos}}{\eta_3}$	$R_6 : HB \rightarrow a_6 = \frac{R_{Vmax} - T_{Vmax}}{\eta_3}$

For each set of input pairs $(\dot{x}_D, \tilde{x})$, the output ν_x is determined by

$$\nu_x = \frac{\sum_{i=1}^{6} f_{M_i}(|\dot{x}_D|) \cdot f_{N_i}(|\tilde{x}|) a_i \tilde{x}}{\sum_{i=1}^{6} f_{M_i}(|\dot{x}_D|) \cdot f_{N_i}(|\tilde{x}|)}, \tag{7}$$

where the term $f_{M_i}(|\dot{x}_D|)$ is the grade of membership of $|\dot{x}_d|$ in each velocity fuzzy set (low and high) and the term $f_{N_i}(|\tilde{x}|)$ is the grade of membership of $|\tilde{x}|$ in each error fuzzy set (small, medium and large).

In the same way, for each set of input pairs $(\dot{y}_D, \tilde{y})$, the output ν_y is determined by

$$\nu_y = \frac{\sum_{i=1}^{6} f_{M_i}(|\dot{y}_D|) \cdot f_{N_i}(|\tilde{y}|) a_i \tilde{y}}{\sum_{i=1}^{6} f_{M_i}(|\dot{y}_D|) \cdot f_{N_i}(|\tilde{y}|)}, \tag{8}$$

where the term $f_{M_i}(|\dot{y}_D|)$ is the grade of membership of $|\dot{y}_d|$ in each velocity fuzzy set (low and high), and the term $f_{N_i}(|\tilde{y}|)$ is the grade of membership of $|\tilde{y}|$ in each error fuzzy set (small, medium and large).

Remark 1. The error η_1 defines the error value from which the designer considers that the robot reaches the trajectory.

Remark 2. The gain a_4 should be high, that is, if the robot is performing a trajectory tracking task, the gain of the controller should be high to reduce the position errors. This practical knowledge is evidenced in the analysis of the stability of the closed-loop system.

Remark 3. The gain a_1 should be small, that is, if the robot is performing a positioning task, the gain of the controller should be small to allow a smooth approximation to the target point.

Remark 4. The error η_2 defines the error value from which the designer considers that the robot should decelerate when approaching low velocity trajectories. The deceleration is due to the small gain a_1.

Remark 5. The error η_3 defines the maximum position error.

3.2. The design of the fuzzy velocity compensators

The fuzzy velocity compensators were specifically designed to limit the control signals and to reduce position errors caused by the difference between the desired values of linear and angular velocities (system inputs) and the current values assumed by the robot.

The reduction of the position errors is achieved changing the gains of the controller between high and small values, whereas the limitation of the control signals is achieved by the gradual change of the gains of the controller as a function of the position error, in such a way that the robot meets the following values of maximum velocity:

- velocity limits for the programmed trajectory:
  $|\dot{x}_D|, |\dot{y}_D| \leq T_{Vmax}$ [m/s];
- velocity limits for the point of interest during a trajectory tracking task:
  $|\dot{x}|, |\dot{y}| \leq R_{Vmax}$ [m/s];
- velocity limits for the point of interest during a positioning task:
  $|\dot{x}|, |\dot{y}| \leq V_{pos}$ [m/s].

The membership functions for the error fuzzy sets are designed using the sector nonlinearity approach. For this reason, such

membership functions are built in a specific way: for $|\tilde{e}| > \eta_1$ [m] only two of the three membership functions can be different from zero and

$$\sum f_{N_i}(|\tilde{e}|) = f_S(|\tilde{e}|) + f_M(|\tilde{e}|) + f_B(|\tilde{e}|) = 1, \tag{9}$$

where $\tilde{e}$ represents the position error $\tilde{x}$ or $\tilde{y}$.

For the same reason, the membership functions for the velocity fuzzy sets should be built such that

$$\sum f_{M_i}(|\dot{v}_D|) = f_L(|\dot{v}_D|) + f_H(|\dot{v}_D|) = 1, \tag{10}$$

where $\dot{v}_D$ represents the velocity $\dot{x}_D$ or $\dot{y}_D$.

Respecting design requirements (9) and (10), for convenience and simplicity the control law given by (3), (7), and (8) can be rewritten as

$$\begin{bmatrix} u_r \\ \omega_r \end{bmatrix} = \mathbf{C}^{-1}\left(\begin{bmatrix} \dot{x}_D \\ \dot{y}_D \end{bmatrix} + \begin{bmatrix} k(\dot{x}_D, \tilde{x}) \cdot \tilde{x} \\ k(\dot{y}_D, \tilde{y}) \cdot \tilde{y} \end{bmatrix}\right), \tag{11}$$

where $k(\dot{x}_D, \tilde{x})$ and $k(\dot{y}_D, \tilde{y})$ are variable gains given by

$$k(\dot{v}_D, \tilde{e}) = \sum_{i=1}^{6} a_i \cdot f_{M_i}(|\dot{v}_D|) \cdot f_{N_i}(|\tilde{e}|). \tag{12}$$

Introducing (11) into (1) one gets the behavior of the velocity of the point of interest for the closed-loop system, that is given by

$$\begin{bmatrix} \dot{x} \\ \dot{y} \end{bmatrix} = \begin{bmatrix} \dot{x}_D + k(\dot{x}_D, \tilde{x}) \cdot \tilde{x} \\ \dot{y}_D + k(\dot{y}_D, \tilde{y}) \cdot \tilde{y} \end{bmatrix}. \tag{13}$$

The gains a_4, a_5 and a_6, and the membership functions $f_S(|\tilde{e}|)$, $f_M(|\tilde{e}|)$ and $f_B(|\tilde{e}|)$ are calculated to limit the velocity of the point of interest of the robot during a trajectory tracking task up to $\dot{x} = \dot{y} = R_{Vmax}$ [m/s], when $\eta_1 \le |\tilde{e}| \le \eta_3$ [m]:

(i) Examining (13) and the velocity limits, one can conclude that

$$k(\dot{v}_D, \tilde{e}) \cdot \tilde{e} = R_{Vmax} - T_{Vmax}. \tag{14}$$

(ii) For $\tilde{e} = \eta_1$ [m] and $\dot{v}_D = T_{Vmax}$ [m/s], the correspondent values of the membership functions are $f_S(|\tilde{e}|) = 1$, $f_M(|\tilde{e}|) = 0$, $f_B(|\tilde{e}|) = 0$, $f_L(|\dot{v}_D|)$ and $f_H(|\dot{v}_D|) = 1$. As a result, according to (12), $k(\dot{v}_D, \tilde{e}) = a_4$. Substituting this gain into (14), one gets that $a_4 \cdot \eta_1 = R_{Vmax} - T_{Vmax}$, therefore, the gain a_4 should be

$$a_4 = \frac{R_{Vmax} - T_{Vmax}}{\eta_1}. \tag{15}$$

(iii) By repeating the previous process for $\tilde{e} = \eta_2$ [m] and $\tilde{e} = \eta_3$ [m], the gains a_5 and a_6 should be

$$a_5 = \frac{R_{Vmax} - T_{Vmax}}{\eta_2} \tag{16}$$

and

$$a_6 = \frac{R_{Vmax} - T_{Vmax}}{\eta_3}. \tag{17}$$

(iv) For $\eta_1 \le \tilde{e} \le \eta_2$ [m] and $\dot{v}_D = T_{Vmax}$ [m/s] the correspondent values of the membership functions are $f_S(|\tilde{e}|) \neq 0$, $f_M(|\tilde{e}|) \neq 0$, $f_B(|\tilde{e}|) = 0$, $f_L(|\dot{v}_D|) = 0$ and $f_H(|\dot{v}_D|) = 1$. Substituting these results into (9) and (12), respectively, one has

$$f_S(|\tilde{e}|) + f_M(|\tilde{e}|) = 1 \tag{18}$$

and

$$k(\dot{v}_D, \tilde{e}) = a_4 \cdot f_S(|\tilde{e}|) + a_5 \cdot f_M(|\tilde{e}|). \tag{19}$$

Substituting (15) and (16) into (19), one gets

$$k(\dot{v}_D, \tilde{e}) = \frac{R_{Vmax} - T_{Vmax}}{\eta_1} \cdot f_S(|\tilde{e}|) + \frac{R_{Vmax} - T_{Vmax}}{\eta_2} \cdot f_M(|\tilde{e}|). \tag{20}$$

Solving the equation system formed by (14), (18), and (20), one gets the membership functions $f_S(|\tilde{e}|)$ and $f_M(|\tilde{e}|)$ for $\eta_1 \le |\tilde{e}| \le \eta_2$ [m], namely

$$f_S(|\tilde{e}|) = \frac{\eta_1}{(\eta_1 - \eta_2)} - \frac{\eta_1 \cdot \eta_2}{(\eta_1 - \eta_2)|\tilde{e}|} \tag{21}$$

and

$$f_M(|\tilde{e}|) = \frac{\eta_1 \cdot \eta_2}{(\eta_1 - \eta_2)|\tilde{e}|} - \frac{\eta_2}{(\eta_1 - \eta_2)}. \tag{22}$$

(v) By repeating the previous process, one gets the membership functions $f_M(|\tilde{e}|)$ and $f_B(|\tilde{e}|)$ for $\eta_2 \le |\tilde{e}| \le \eta_3$ [m], namely

$$f_M(|\tilde{e}|) = \frac{\eta_2}{(\eta_2 - \eta_3)} - \frac{\eta_2 \cdot \eta_3}{(\eta_2 - \eta_3)|\tilde{e}|} \tag{23}$$

and

$$f_B(|\tilde{e}|) = \frac{\eta_2 \cdot \eta_3}{(\eta_2 - \eta_3)|\tilde{e}|} - \frac{\eta_3}{(\eta_2 - \eta_3)}. \tag{24}$$

The gains a_2 and a_3 are calculated to limit the velocity of the point of interest of the robot up to $\dot{x} = \dot{y} = V_{pos}$ [m/s] when $\eta_2 \le |\tilde{e}| \le \eta_3$ [m], during a positioning task ($\dot{x}_D = \dot{y}_D = 0$ [m/s]). By repeating a similar process, the gains a_2 and a_3 should be

$$a_2 = \frac{V_{pos}}{\eta_2} \tag{25}$$

and

$$a_3 = \frac{V_{pos}}{\eta_3}. \tag{26}$$

3.3. Stability analysis

Taking into account the dynamic of the robot, the stability of the system is analyzed under the assumption of imperfect velocity tracking, that is $u \neq u_r$ and $\omega \neq \omega_r$. Considering the velocity tracking errors, it can be written that

$$\begin{bmatrix} u \\ \omega \end{bmatrix} = \begin{bmatrix} u_r \\ \omega_r \end{bmatrix} - \begin{bmatrix} \varepsilon_u \\ \varepsilon_\omega \end{bmatrix}, \tag{27}$$

where ε_u and ε_ω are, respectively, the differences between the kinematic commands and the effective linear and angular velocities developed by the robot. Introducing (27) into (1), the closed-loop system equation becomes

$$\begin{bmatrix} \dot{\tilde{x}} \\ \dot{\tilde{y}} \end{bmatrix} = -\begin{bmatrix} k_x(\dot{x}_D, \tilde{x}) \cdot \tilde{x} \\ k_y(\dot{y}_D, \tilde{y}) \cdot \tilde{y} \end{bmatrix} + \mathbf{C}\begin{bmatrix} \varepsilon_u \\ \varepsilon_\omega \end{bmatrix}. \tag{28}$$

Proposing the Lyapunov candidate function

$$V = \frac{1}{2}\begin{bmatrix} \tilde{x} \\ \tilde{y} \end{bmatrix}^T \begin{bmatrix} \tilde{x} \\ \tilde{y} \end{bmatrix} > 0,$$

a sufficient condition for the stability of the equilibrium of the closed-loop system is that

$$\dot{V} = \tilde{x} \cdot \dot{\tilde{x}} + \tilde{y} \cdot \dot{\tilde{y}} < 0. \tag{29}$$

Introducing (28) into (29), one gets

$$\dot{V} = -\tilde{x}^2 \cdot k_x(\dot{x}_D, \tilde{x}) - \tilde{y}^2 \cdot k_y(\dot{y}_D, \tilde{y}) + \tilde{x}[\varepsilon_u \cos(\psi) - a\varepsilon_\omega \sin(\psi)] + \tilde{y}[\varepsilon_u \sin(\psi) + a\varepsilon_\omega \cos(\psi)]. \tag{30}$$

Choosing only positive gains a_i, $k_x(\dot{x}_D,\tilde{x})>0$ and $k_y(\dot{y}_D,\tilde{y})>0$. Therefore, a sufficient condition for (30) to become negative is

$$\tilde{x}^2 \min\{k_x(\dot{x}_D,\tilde{x})\} > |\tilde{x}[\varepsilon_u \cos(\psi) - a\varepsilon_\omega \sin(\psi)]| \quad (31)$$

and

$$\tilde{y}^2 \min\{k_y(\dot{y}_D,\tilde{y})\} > |\tilde{y}[\varepsilon_u \sin(\psi) + a\varepsilon_\omega \cos(\psi)]|. \quad (32)$$

Thus, since $a_i \in \Re^+$, the system stability is guaranteed with control errors ultimately bounded by

$$|\tilde{x}| < \frac{|\varepsilon_u \cos(\psi) - a\varepsilon_\omega \sin(\psi)|}{\min\{k_x(\dot{x}_D,\tilde{x})\}} \quad (33)$$

and

$$|\tilde{y}| < \frac{|\varepsilon_u \sin(\psi) + a\varepsilon_\omega \cos(\psi)|}{\min\{k_y(\dot{y}_D,\tilde{y})\}}. \quad (34)$$

Notice that (33) and (34) evidence that high gains reduce the position errors.

Remark 6. In the case of a perfect velocity tracking, that is, with $\varepsilon_u = 0$ and $\varepsilon_\omega = 0$, the ultimate bounds of Eqs. (33) and (34) are zero, then

$$\tilde{x} \to 0 \quad \text{and} \quad \tilde{x} \to 0, \quad (35)$$

and the closed-loop system is asymptotically stable.

Now, considering that a fixed target point is chosen to position the robot, that is, with

$$\dot{x}_D = 0 \quad \text{and} \quad \dot{y}_D = 0, \quad (36)$$

and substituting (35) and (36) into (11), one gets asymptotically that

$$\begin{bmatrix} u_r \\ \omega_r \end{bmatrix} = \begin{bmatrix} 0 \\ 0 \end{bmatrix}. \quad (37)$$

This means that when the robot reaches the target point both control signals become zero, and the robot stays in that position. Therefore, the proposed controller can also be used to position the robot without orientation control.

4. Experimental results

In this section, three experiments are reported to demonstrate the operation of the proposed controller. Furthermore, the performance of the proposed controller is compared with the performance of the controller proposed in Martins et al. (2008) where a fixed saturation function is used to limit the control actions.

To comply with the objective of the trajectory tracking, Martins et al. (2008) propose the control law

$$\begin{bmatrix} u_r \\ \omega_r \end{bmatrix} = \mathbf{C}^{-1}\left(\begin{bmatrix} \dot{x}_D \\ \dot{y}_D \end{bmatrix} + \begin{bmatrix} l_x \tanh(\frac{k_x}{l_x}\tilde{x}) \\ l_y \tanh(\frac{k_y}{l_y}\tilde{y}) \end{bmatrix} \right), \quad (38)$$

where u_r and ω_r are the controller outputs; $\dot{x}_D$ and $\dot{y}_D$ are, respectively, the projection of the velocity of the desired trajectory in the X and Y directions of the fixed frame; $l_x > 0$ and $l_y > 0$ are saturation constants; and $k_x > 0$ and $k_y > 0$ are the gains of the controller. In this control law, the saturation of the control signals is guaranteed using the hyperbolic tangent. The suitable values of the saturation constants shall be $l_x = l_y = R_{Vmax} - T_{Vmax}$.

The controllers were implemented on a Pioneer 3-DX mobile robot using the development software supplied by the manufacturer. A sampling period of 0.1 s was used in the experiments. Fig. 5 shows the robot used and a view of the experimental indoor environment.

Taking into consideration the workspace of the robot the following velocity limits were established for running the experiments: $T_{Vmax} = 0.3$ m/s, $R_{Vmax} = 0.4$ m/s and $V_{pos} = 0.3$ m/s.

To design the controller with velocity limitation via fuzzy gains it was chosen as $\eta_1 = 0.025$ m, $\eta_2 = 0.3$ m, $\eta_3 = 20$ m and $a_1 = 2$. Consequently, according to the velocity limits established and the design criteria given in Section 3, the other parameters of the

Fig. 5. The robot used into the experimental environment.

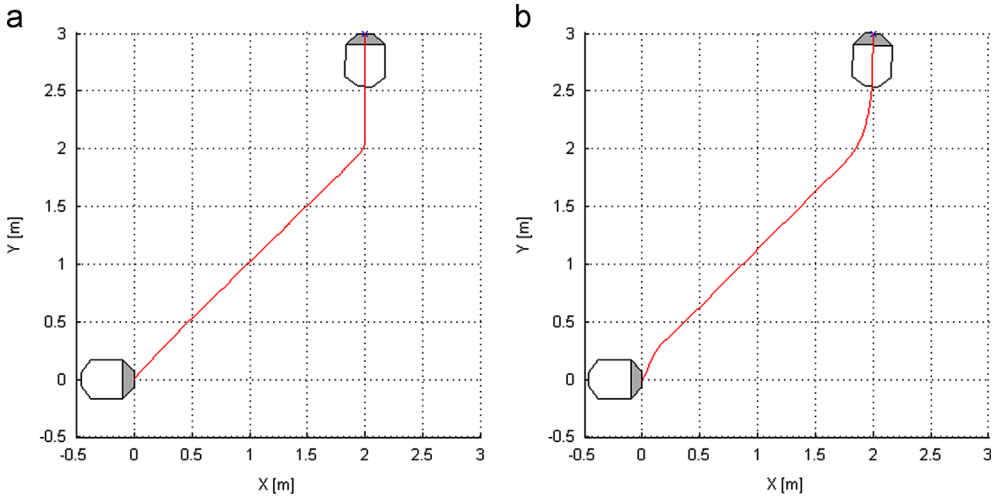

Fig. 6. First experiment: (a) path followed by the robot using the controller with fixed saturation function; (b) path followed by the robot using the proposed controller.

controller shall be $a_2 = 1$, $a_3 = 3/200$, $a_4 = 4$, $a_5 = 1/3$ and $a_6 = 1/200$.

As for the trajectory tracking controller with velocity limitation via hyperbolic tangent, it was chosen as $k_x = k_y = 2$ (such gains were chosen after running several experiments) and the saturation constants shall be $l_x = l_y = 0.1$ due to velocity limits established.

4.1. First experiment

In the first experiment, corresponding to a positioning task, the robot should reach the point $x=2$ m, $y=3$ m, starting from the initial pose $x=0$ m, $y=0$ m with $\psi = 0^\circ$.

Fig. 6 shows the path navigated by the robot to reach the target point, using the controller with limitation via hyperbolic tangent and with fuzzy gains. One can notice that the robot follows a smoother path using the proposed controller than using the controller with limitation via hyperbolic tangent, despite the velocity of the robot being higher using the controller proposed here.

Fig. 7 shows the evolution of the magnitude of the velocity of the point of interest, using the two controllers. For the controller with limitation via hyperbolic tangent, one can notice that the velocity of the point of interest is limited to 0.142 m/s. This limitation occurs because it is necessary to impose $l_x = l_y = 0.1$ as saturation constants for such controller to ensure that the velocity bound will be respected. In turn, using the controller with limitation via fuzzy gains, one can notice that the velocity of the point of interest is limited to 0.426 m/s, even respecting the same velocity limits.

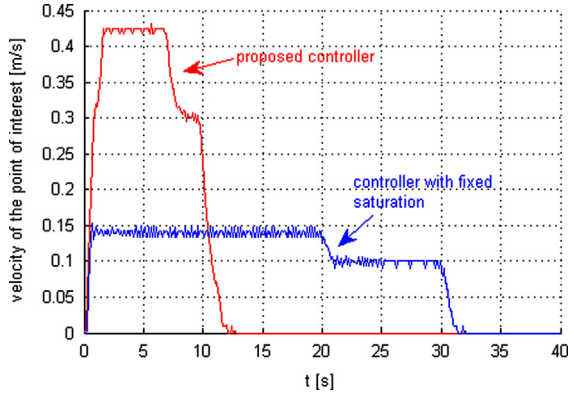

Fig. 7. Evolution of the magnitude of the velocity of the point of interest during the first experiment.

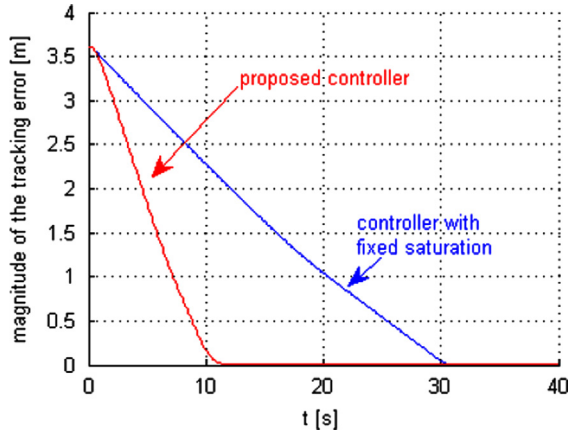

Fig. 8. Evolution of the magnitude of the tracking error during the first experiment.

Fig. 8 shows the evolution of the magnitude of the tracking error using the two controllers, which is used to calculate the performance metrics for this experiment. One can notice that the proposed task is accomplished in less time by the controller proposed here.

Fig. 9 presents the curve correspondent to the velocity of the point of interest in the X direction versus position error in the X direction. Notice, firstly, that the velocity of the point of interest in the X direction is limited to $V_{pos} = 0.3$ m/s, as expected. Secondly, notice that the robot travels 0.2 m in the X direction to reach cruising velocity due to its dynamics and, thirdly, notice that the dynamics of the robot is respected by the controller proposed here which decreases the velocity of the robot in the X direction from the error $\eta_2 = 0.3$ m to get a suitable arrival of the robot at the target point.

4.2. Second experiment

In the second experiment, correspondent to a trajectory tracking task, the robot should follow the trajectory defined by

$$p_2(t) = (x_D(t)(=0.2 \cdot t, y_D(t)(=1),$$

starting from the initial pose $x=0$ m, $y=0$ m with $\psi = 0^\circ$.

Fig. 10 presents the reference and real trajectories for the experiment, using the two controllers. Fig. 11 shows the evolution of the magnitude of the tracking error using both controllers, which is used to calculate the performance metrics for the experiment. One can notice that the robot reaches the trajectory in less time when using the proposed controller.

4.3. Third experiment

In the third experiment, also correspondent to a trajectory tracking task, the robot should follow the eight-shaped trajectory defined by

$$p_3(t) = (x_D(t) = 1 \cdot \sin(0.3 \cdot t), y_D(t) = 1 \cdot \cos(0.15 \cdot t) - 1),$$

starting from the initial pose $x=0$ m, $y=0$ m with $\psi = 0^\circ$.

Fig. 12 presents the reference trajectory and the trajectory performed by the robot for the experiment, using the two controllers. Fig. 13(a) shows the evolution of the magnitude of the tracking error using both controllers and Fig. 13(b) shows a detail of such evolution. One can notice in Fig. 13(b) that the magnitude of the tracking error is smaller when using the proposed controller.

4.4. Analysis of the experiments and performance comparison

The performance of the controllers was evaluated based on two consolidated criteria, the IAE (Integral of Absolute Error) and the ITAE (Integral of Time Multiplied by Absolute Error), which are

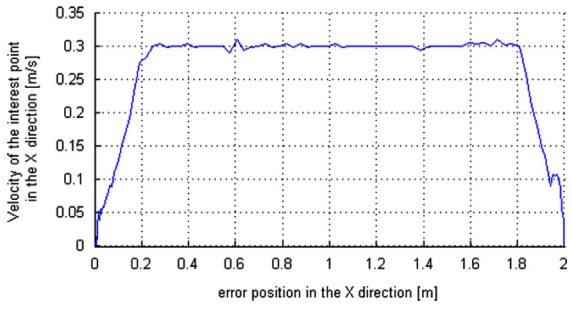

Fig. 9. Curve velocity of the point of interest in the X direction versus error in the X direction.

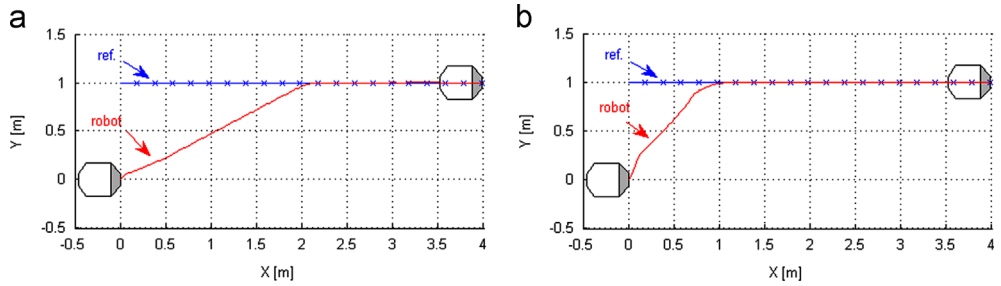

Fig. 10. Second experiment: (a) reference and real trajectories using the controller with fixed saturation function; (b) reference and real trajectories using the proposed controller.

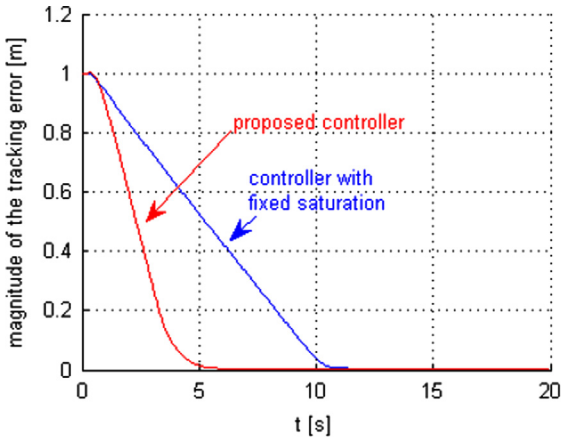

Fig. 11. Evolution of the magnitude of the tracking error during the second experiment.

calculated as

$$IAE = \int_{T_1}^{T_2} |E(t)| \cdot dt, \quad E(t) = \sqrt{\tilde{x}^2 + \tilde{y}^2} \tag{39}$$

and

$$ITAE = \int_{T_1}^{T_2} t \cdot |E(t)| \cdot dt, \quad E(t) = \sqrt{\tilde{x}^2 + \tilde{y}^2}, \tag{40}$$

where $E(t)$ is the instantaneous value of the trajectory tracking error, t is the time, and T_1 and T_2 define the time interval for the calculation of the two metrics.

Table 2 presents the values of IAE and ITAE obtained for each experiment. Analyzing such values, one can conclude that the nonlinear trajectory tracking controller with velocity limitation via fuzzy gains has superior performance, compared to the nonlinear trajectory tracking controller with velocity limitation via hyperbolic tangent, mainly in the execution of the positioning tasks (first experiment) and trajectory tracking tasks, requiring the approximation of the robot to the desired trajectory (second experiment). The trajectory tracking controller with fuzzy gains is also slightly more efficient when performing tasks of trajectory tracking with sudden changes of velocity and direction (third experiment).

5. Conclusions

This paper proposes and validates a new nonlinear trajectory tracking controller for unicycle-like robots. The proposed controller uses fuzzy rules to determine the gains of the nonlinear controller, according to the values of the velocities of the reference trajectory and the values of the tracking errors. Such fuzzy rules were designed aiming at limiting the control signals, as well as reducing the errors arising from the robot dynamics.

The proposed controller was implemented in a commercial robot Pioneer 3-DX, and experimental results were presented, showing that the robot is capable of tracking a desired trajectory with a small distance error. The proposed controller was also compared to a controller with fixed saturation function, which uses the hyperbolic tangent to limit the control signals, and experimental results showed that it has superior performance.

The proposed controller is easy to implement, making it suitable for implementation in low-profile processors, and its control inputs

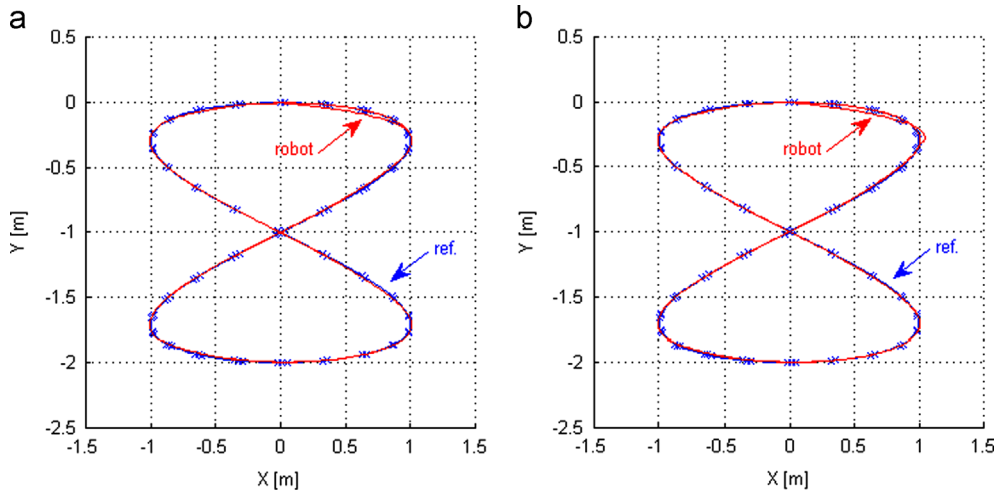

Fig. 12. Third experiment: (a) reference trajectory and the trajectory performed by the robot using the controller with fixed saturation function; (b) reference trajectory and the trajectory performed by the robot using the proposed controller.

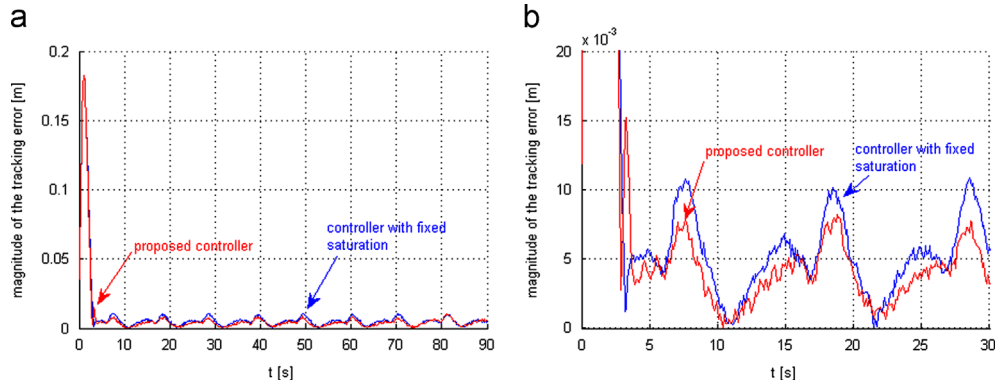

Fig. 13. Third experiment: (a) evolution of the magnitude of the tracking error; (b) detail of the evolution of the magnitude of the tracking error.

Table 2
The obtained values of IAE and ITAE for the experiments.

Experiment	IAE		ITAE	
	Fixed saturation	Fuzzy gains	Fixed saturation	Fuzzy gains
First	51.4	19.0	499.9	64.6
Second	5.3	2.4	18.5	3.5
Third	1.07	1.01	28.83	24.79

are the linear and angular velocities, common to most commercial robots. It provides an appropriate value for robot velocity commands, avoiding saturation values of control signals, while keeping a good performance of the control system. Finally, the stability of the closed-loop system is analyzed and confirmed using the Lyapunov theory, ensuring that the task being performed will be accomplished accordingly.

References

Andaluz, V., Roberti, F., Toibero, J. M., & Carelli, R. (2012). Adaptive unified motion control of mobile manipulators. *Control Engineering Practice*, *20*(12), 1337–1352.

Antonelli, G., Chiaverini, S., & Fusco, G. (2007). A fuzzy-logic-based approach for mobile robot path tracking. *IEEE Transactions on Fuzzy Systems*, *15*(2), 211–221.

Deist, L., & Fourie, C. (1993). Fuzzy algorithm for the control of a mobile robot. In *International workshop on emerging technologies and factory automation* (pp. 42–50), September.

Guechi, E., Lauber, J., Dambrine, M., Klancar, G., & Blazic, S. (2010). Pdc control design for non-holonomic wheeled mobile robots with delayed outputs. *Journal of Intelligent & Robotic Systems*, *60*(December (3)), 395–414.

Guechi, E.-H., Abellard, A., & Franceschi, M. (2012). Experimental fuzzy visual control for trajectory tracking of a khepera ii mobile robot. In: *IEEE international conference on industrial technology* (*ICIT*) (pp. 25–30), March.

Hung, L.-C., & Chung, H.-Y. (2006). Design of hierarchical fuzzy logic control for mobile robot system. In *IEEE conference on robotics, automation and mechatronics* (pp. 1–6).

Lakehal, B., Amirat, Y., & Pontnau, J. (1995). Fuzzy steering control of a mobile robot. In *International IEEE/IAS conference on industrial automation and control* (pp. 383–386), May.

Mamdani, E. (1974). Application of fuzzy algorithms for control of simple dynamic plant. *Proceedings of the Institution of Electrical Engineers*, *121*(12), 1585–1588.

Martins, F. N., Celeste, W. C., Carelli, R., Sarcinelli-Filho, M., & Bastos-Filho, T. F. (2008). An adaptive dynamic controller for autonomous mobile robot trajectory tracking. *Control Engineering Practice*, *16*(11), 1354–1363.

Resende, C. Z., Espinosa, F., Bravo-Muñoz, I., Sarcinelli-Filho, M., & Bastos-Filho, T. F. (2011). A trajectory tracking controller with dynamic gains for mobile robots. In *IEEE/RSJ international conference on intelligent robots and systems* (pp. 3746–3751).

Susnea, I., Filipescu, A., Vasiliu, G., & Filipescu, S. (2008). Path following, real-time, embedded fuzzy control of a mobile platform wheeled mobile robot. In *IEEE international conference on automation and logistics* (pp. 268–272).

Takagi, T., & Sugeno, M. (1985). Fuzzy identification of systems and its applications to modelling and control. *IEEE Transactions on Systems Man and Cybernetics*, *SMC-15*(1), 116–132.

Tanaka, K., Kosaki, T., & Wang, H. O. (1998). Backing control problem of a mobile robot with multiple trailers: *Fuzzy modeling and lmi-based design*. *IEEE Transactions on Systems Man and Cybernetics C, Applications and Reviews*, *28*(August (3)), 329–337.

Tanaka, K., & Sugeno, M. (1992). Stability analysis and design of fuzzy control systems. *IEEE Transactions on Fuzzy Systems*, *45*(2), 135–156.

Tanaka, K. & Wang, H. O. (2001). *Fuzzy control systems design and analysis: A linear matrix inequality approach*. John Wiley & Sons, Inc. ISBN-10: 0471323241.

Wang, H., Tanaka, K., & Griffin, M. (1996). An approach to fuzzy control of nonlinear systems: *Stability and design issues*. *IEEE Transactions on Fuzzy Systems*, *4* (February (1)), 14–23.

Zadeh, L. A. (1973). Outline of a new approach to the analysis of complex systems and decision processes. *IEEE Transactions on Systems Man and Cybernetics*, *SMC-3*(1), 28–44.